Cdc13p: A Single-Strand Telomeric DNA–Binding Protein with a Dual Role in Yeast Telomere Maintenance

Constance I. Nugent,* Timothy R. Hughes,* Neal F. Lue, Victoria Lundblad†

The *CDC13* gene has previously been implicated in the maintenance of telomere integrity in *Saccharomyces cerevisiae*. With the use of two classes of mutations, here it is shown that *CDC13* has two discrete roles at the telomere. The *cdc13-2^{est}* mutation perturbs a function required in vivo for telomerase regulation but not in vitro for enzyme activity, whereas *cdc13-1^{ts}* defines a separate essential role at the telomere. In vitro, purified Cdc13p binds to single-strand yeast telomeric DNA. Therefore, Cdc13p is a telomere-binding protein required to protect the telomere and mediate access of telomerase to the chromosomal terminus.

The activity of the telomerase enzyme, which replicates telomeres, has been proposed to be a determinant of the replicative potential of cells (*1*, *2*). Cells without the ability to replicate their chromosomal termini gradually shorten their telomeres and eventually exhibit cellular senescence (*3*, *4*). However, telomerase activity is present in some human cell lines (*5*) that display telomere shortening (*1*, *6*), which suggests that regulatory factors control this enzyme in vivo. Information is lacking about the regulation of this enzyme and how telomerase interacts with proteins present at the chromosomal terminus as both telomerase and single-strand telomeric DNA–binding proteins have not been identified in a genetically manipulatable system such as yeast.

We have screened for mutants of *S. cerevisiae* with a phenotype similar to a telomerase defect and have identified four genes: the previously identified *EST1* gene (*EST*, ever shorter telomeres) (*7*) and three additional genes, *EST2*, *EST3*, and *EST4* (*8*). Mutations in these genes result in phenotypes that are virtually identical to those observed when a known component of telomerase, the yeast telomerase RNA *TLC1* gene (*3*), is deleted: telomeres become progressively shorter and each mutant strain displays a senescence phenotype. In addition, multiple mutant combinations between the *TLC1* and *EST* genes show no enhancement of phenotype relative to that displayed by any single mutant strain (*8*). This finding implies that the four *EST* genes encode either components of telomerase or other factors that are required in vivo for the telomerase pathway.

The *EST4* locus was represented by a single allele, *est4-1*. Cloning of the wild-type gene by complementation of the senescence and telomere phenotypes of the *est4-1* strain identified several genomic clones containing the previously identified *CDC13* gene (*9*). Plasmid gap repair of the *est4-1* mutation localized the mutation to a region internal to the *CDC13* gene. Genomic replacement in a wild-type strain with the gap-repaired mutant allele resulted in a strain that was phenotypically identical to the original *est4-1* strain (*10*); this demonstrated that the *est4-1* mutation was a novel

C. I. Nugent, T. R. Hughes, V. Lundblad, Department of Molecular and Human Genetics and Cell and Molecular Biology Program, Baylor College of Medicine, Houston, TX 77030, USA.
N. F. Lue, Department of Microbiology, Cornell Medical College, New York, NY 10021, USA.

*These authors contributed equally to this work.
†To whom correspondence should be addressed.

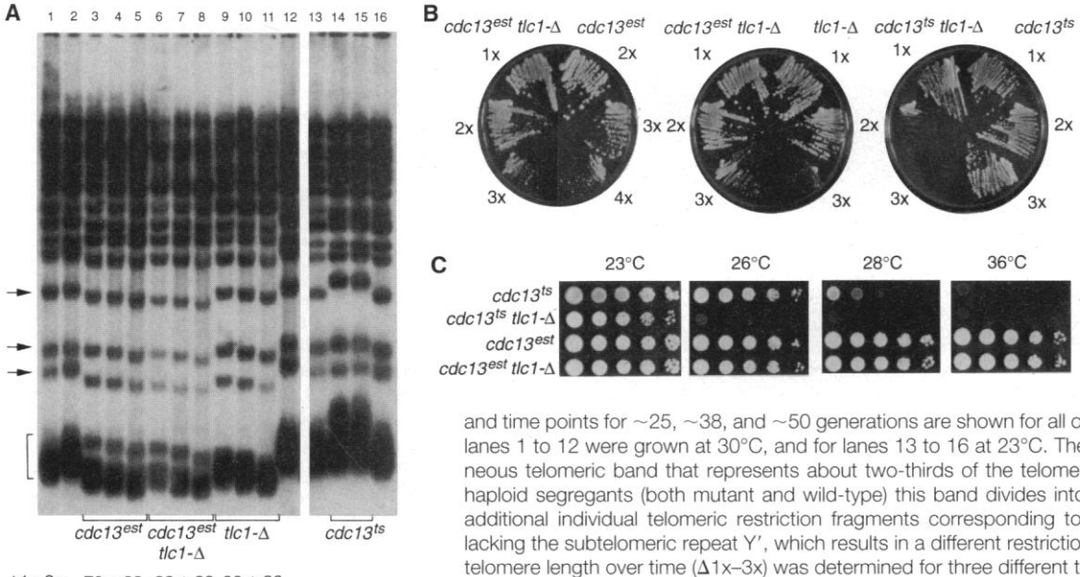

Fig. 1. The *cdc13-1^{ts}* and *cdc13-2^{est}* mutations behave differently in a *tlc1-Δ* strain. (**A**) Southern blots to assess telomere-shortening phenotypes, using a poly-[d(GT/CA)] probe, were performed as described (*7*). Lane 1, *cdc13-2^{est}/CDC13*, *tlc1-Δ::LEU2/TLC1* diploid parent to the haploid strains in lanes 2 to 12. Lanes 2, 12, 13, and 16, *CDC13^{+} TLC1^{+}*. Time points for ~25 and ~50 generations of growth are shown for the *CDC13^{+} TLC1^{+}* and *cdc13-1^{ts}* strains, and time points for ~25, ~38, and ~50 generations are shown for all other strains (*28*). The strains for lanes 1 to 12 were grown at 30°C, and for lanes 13 to 16 at 23°C. The bracket indicates a heterogeneous telomeric band that represents about two-thirds of the telomeres in this strain; in occasional haploid segregants (both mutant and wild-type) this band divides into two subbands. Arrows show additional individual telomeric restriction fragments corresponding to a second class of telomeres lacking the subtelomeric repeat Y′, which results in a different restriction pattern (*29*). The reduction in telomere length over time (Δ1x–3x) was determined for three different telomeres, for five to six haploid strains for each genotype (*30*). (**B**) Isogenic freshly germinated spores with the indicated genotypes (*28*) were examined for progressive growth defects by streaking for single colonies three to four times in succession on rich-media plates incubated at 23°C. A total of 15 to 31 different isolates were examined for each genotype from four to six different experiments; although similar results were always obtained for each genotype, it is difficult to more quantitatively assess this phenotype. Each time point represents ~25 generations of growth (1x, 2x, and 3x correspond to ~25, ~50, and ~75 generations of growth, although this is an approximate estimate because of the difficulty of accurately determining the number of cell divisions in a rapidly senescing strain). Because the senescence phenotype of *cdc13-2^{est}* is slightly delayed relative to that of the null *tlc1-Δ* mutation (*8*), the time points of the *cdc13-2^{est}* streakouts displayed here are offset by ~25 generations relative to the other streakouts. (**C**) Dilutions of strains of the indicated genotypes were spotted on rich media and grown at the indicated temperatures.

allele of *CDC13*, referred to hereafter as *cdc13-2*^{est}. The *CDC13* gene had previously been implicated in telomere function, as suggested by the rapid loss of one strand of the telomere that occurs in a *cdc13-1*^{ts} strain at nonpermissive temperatures (*9*, *11*). However, *cdc13-2*^{est} exhibited none of the conditional lethality or cell-cycle arrest phenotypes of the *cdc13-1*^{ts} strain (*12*), and extensive single-strand telomeric DNA was not observed in the *cdc13-2*^{est} mutant (*13*). The identification of two alleles of *CDC13* (*14*) with distinct phenotypes suggested that this gene has two discrete functions.

To investigate whether these two mutations altered different aspects of telomere function, we eliminated the telomerase RNA gene (*TLC1*) in *cdc13-1*^{ts} and *cdc13-2*^{est} strains. A *cdc13-2*^{est} *tlc1*-Δ double mutant strain exhibited the same degree of telomere shortening as displayed by either *tlc1*-Δ (telomerase-minus) or *cdc13-2*^{est} single mutants, and all three strains had similar senescence phenotypes (Fig. 1, A and B). The lack of an enhancement of phenotype in the double mutant suggests that *cdc13-2*^{est} perturbs a function of *CDC13* that is required for the telomerase pathway. In contrast, a synthetic phenotype was observed in a *tlc1*-Δ strain that also contained the *cdc13-1*^{ts} allele. Alone, the *cdc13-1*^{ts} strain did not exhibit either senescence or telomere shortening at 23°C (*15*), but this strain was inviable above 26°C (Fig. 1C) (*16*). However, the *cdc13-1*^{ts} *tlc1*-Δ double mutant strain was inviable above 23°C (Fig. 1C), and the senescence behavior of this strain was exaggerated relative to that of a *tlc1*-Δ strain (Fig. 1B). Therefore, the *cdc13-1*^{ts} allele alters a separate aspect of Cdc13p that is required for maintaining the telomere in conjunction with telomerase.

The similarity in phenotypes displayed by the *tlc1*-Δ and *cdc13-2*^{est} mutant strains suggested that telomerase activity, which is eliminated in a *tlc1*-Δ strain (*17*), might also be affected in the *cdc13-2*^{est} strain. However, in extracts prepared from the *cdc13-2*^{est} strain (*18*), telomerase activity was present in amounts comparable to that exhibited by a wild-type strain, whereas activity was absent in extracts from a strain

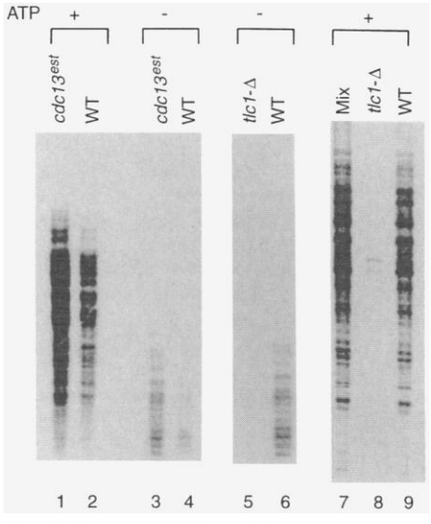

Fig. 2. The *cdc13-2*^{est} mutation does not eliminate telomerase activity in vitro. Yeast telomerase assays using column fractions (*18*) were assayed as described (*26*), except that [α-^{32}P]deoxythymidine triphosphate (3000 Ci/mmol, 0.3 mM) and deoxyguanosine triphosphate (50 mM) were used as the nucleotide triphosphate substrates. Lane 7 is a mixture of *tlc1*-Δ and *TLC1*$^{+}$ (WT) extracts. Reactions in lanes 1, 2, 7, 8, and 9 were done in the presence of 1 mM adenosine triphosphate (ATP), which stimulates yeast telomerase processivity (*26*). The *cdc13-2*^{est} and *CDC13*$^{+}$ strains were isogenic to those used in Fig. 1 (*28*); the *tlc1*-Δ and *TLC1*$^{+}$ genotypes were assayed in a protease-deficient strain background.

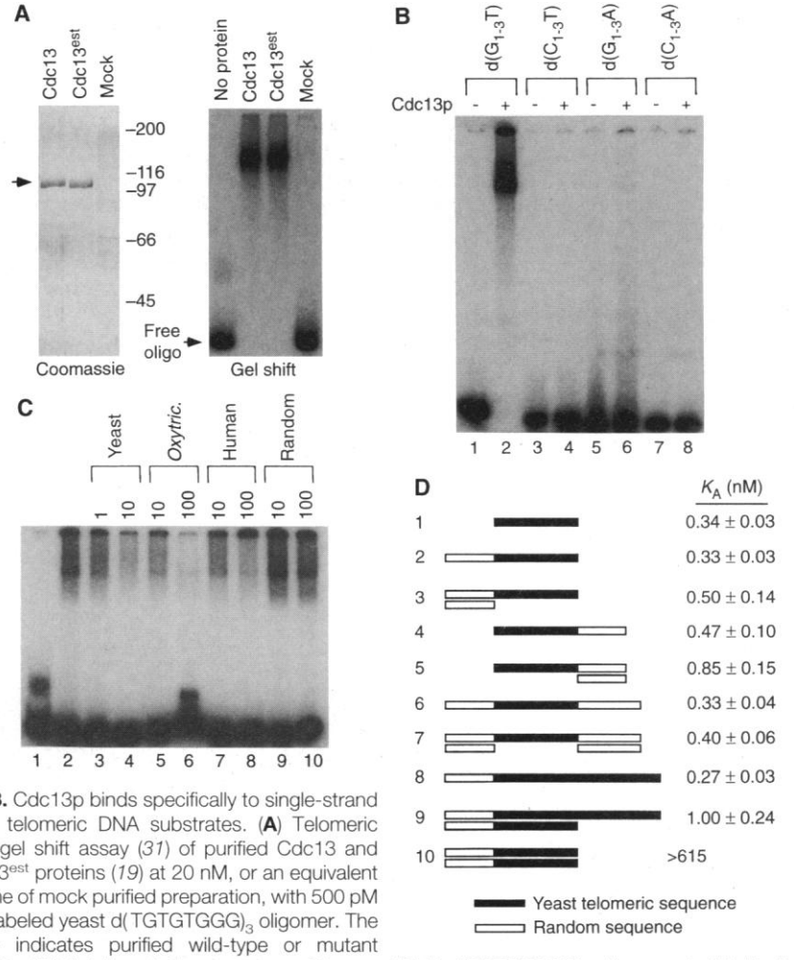

Fig. 3. Cdc13p binds specifically to single-strand yeast telomeric DNA substrates. (**A**) Telomeric DNA gel shift assay (*31*) of purified Cdc13 and Cdc13^{est} proteins (*19*) at 20 nM, or an equivalent volume of mock purified preparation, with 500 pM end-labeled yeast d(TGTGTGGG)$_3$ oligomer. The arrow indicates purified wild-type or mutant Cdc13p. (**B**) Variations in the sequence of the yeast DNA d(TGTGTGGG)$_3$ oligomer abolish binding; all oligomers were at 500 pM, and 50 nM Cdc13p was added, as indicated. (**C**) Telomeric DNA gel shift assays of Cdc13p (50 nM) in the presence of various competitors, with 500 nM labeled d(TGTGTGGG)$_3$ oligomer (lane 1, no protein added; lane 2, no competitor added). Unlabeled competitors were added at a molar excess of 1, 10, or 100, as indicated, relative to the labeled d(TGTGTGGG)$_3$ oligomer [*Oxytricha* telomeric oligomer, d(T$_4$G$_4$)$_3$; human telomeric oligomer, d(T$_2$AG$_3$)$_4$; random-sequence oligomer, d(AGCGGATAACAATTTCACACAGGA)]. The additional band appearing in lanes 1 and 6 is an intermolecular structure that forms as a result of the high oligonucleotide concentrations used in these substrate-excess mobility shifts. Oligonucleotide secondary structure is not required for Cdc13p binding, on the basis of criteria including tolerance to lithium ions and affinity for sequences that do not readily form secondary structures (*20*). (**D**) Apparent binding affinity constant (K_A) values of Cdc13p binding to a panel of substrate variants. Substrates 1 to 7 and 10 contain 24 nucleotides (nt), and substrates 8 and 9 contain 48 nt, respectively, of d(G$_{1-3}$T) sequences; random sequences were 15 nt long, except for substrates 6 and 7, with 20 nt on the 3′ end. Means and SDs shown represent half-binding points, with a dilution series of Cdc13p and oligonucleotide concentration fixed at 20 pM, in three separate gel-shift experiments involving two protein preparations, as quantitated by PhosphorImager analysis (*31*). Increased incubation time or reduced oligonucleotide concentrations did not alter binding characteristics (*20*), indicating that equilibrium was achieved and oligonucleotide concentration was sufficiently low.

deleted for *TLC1* (Fig. 2). These data show that the *cdc13-2^{est}* mutation defines a function of *CDC13* that is required in vivo for regulation of telomerase but not in vitro for enzyme activity.

Although Cdc13p does not have sequence features that would suggest it is a DNA-binding protein, the appearance of single-strand telomeric DNA that occurs in the *cdc13-1^{ts}* strain (*9*, *11*) could be the result of the loss of a *CDC13*-encoded telomere-binding activity. To test this hypothesis, we assessed the ability of purified Cdc13p (*19*) to bind yeast telomeric substrates. As assayed by gel mobility shifts, Cdc13p bound to several single-strand G-rich yeast telomeric oligomers, with a binding affinity of ~0.3 nM (Fig. 3, A and D). No binding was observed to five random-sequence oligomers of equivalent size (*20*), and conversion of the yeast deoxynucleotide oligomer $d(G_{1-3}T)$ to $d(C_{1-3}A)$, $d(C_{1-3}T)$, or $d(G_{1-3}A)$ abolished binding (Fig. 3B). However, Cdc13p was capable of binding to human and ciliate G-rich telomeric sequences (Fig. 3C), although its binding affinity was about one-tenth of that for yeast substrates (*21*). Although binding to fully duplex telomeric substrates was greatly reduced, Cdc13p bound equally well to a number of partially duplex substrates, which indicates that binding does not require a free 3′ terminus and is not enhanced by duplex telomeric DNA at the 5′ end (Fig. 3D). Although this result implies that Cdc13p binding alone is not specific for the very end of the chromosome, Cdc13p genetically interacts with another single-strand telomeric DNA–binding protein, Est1p (*22*), which does require a free 3′ terminus for binding (*23*).

Single-strand telomeric DNA–binding proteins have been identified in the ciliates and *Xenopus* (*24*), but it has not been possible to test their role in telomerase regulation in vivo. We propose that Cdc13p is a yeast single-strand telomeric DNA–binding protein and that this protein functions in two distinct roles at the telomere (Fig. 4). First, Cdc13p is required to protect the end of the chromosome, which is essential for cell viability. Second, Cdc13p serves as a positive regulator of telomerase by mediating access of the enzyme to the chromosomal terminus; this telomerase-loading activity is abolished by the *cdc13-2^{est}* mutation. Consistent with this model, the Cdc13^{est} mutant protein binds telomeric DNA (Fig. 3A), and extracts from *cdc13-2^{est}* mutant strains have wild-type amounts of telomerase activity (Fig. 2). Previous studies on the connection between telomere length maintenance and cellular senescence have focused on telomerase as a primary determinant of cellular replicative capacity (*3*, *4*, *25*). Our results demonstrate that components of telomeric chromatin can also play a critical role in determining the senescence process. Regulation of telomerase in mammalian systems (*1*, *5*, *6*) may also require factors similar to those described here.

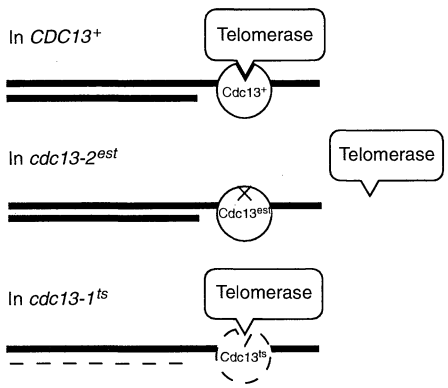

Fig. 4. A model for regulation of telomerase by a telomere-binding protein. Cdc13p is shown bound to the single-strand G-rich extension present at the end of the chromosome (*32*), both protecting the chromosome end from degradation and mediating telomerase action. Telomerase access could occur by a direct interaction between Cdc13p and the enzyme, as shown, or through an intermediary protein. In the *cdc13-2^{est}* mutant, telomerase access is compromised; in the *cdc13-1^{ts}* mutant, protection from degradation is lost.

REFERENCES AND NOTES

1. H. J. Cooke and B. A. Smith, *Cold Spring Harbor Symp. Quant. Biol.* **51**, 213 (1986).
2. C. B. Harley, A. B. Futcher, C. W. Greider, *Nature* **345**, 458 (1990); N. D. Hastie *et al.*, *ibid.* **346**, 866 (1990).
3. M. S. Singer and D. E. Gottschling, *Science* **266**, 404 (1994).
4. G.-L. Yu, J. D. Bradley, L. D. Attardi, E. H. Blackburn, *Nature* **344**, 126 (1990); J. Feng *et al.*, *Science* **269**, 1236 (1995).
5. D. Broccoli, T. W. Young, T. de Lange, *Proc. Natl. Acad. Sci. U.S.A.* **92**, 9082 (1995); C. M. Counter, J. Gupta, C. B. Harley, B. Leber, S. Bacchetti, *Blood* **85**, 2315 (1995); K. Hiyama *et al.*, *J. Immunol.* **155**, 3711 (1995).
6. R. C. Allshire *et al.*, *Nature* **332**, 656 (1988); T. de Lange *et al.*, *Mol. Cell. Biol.* **10**, 518 (1990).
7. V. Lundblad and J. W. Szostak, *Cell* **57**, 633 (1989).
8. T. Lendvay, D. K. Morris, J. Sah, B. Balasubramanian, V. Lundblad, *Genetics*, in press.
9. B. Garvik, M. Carson, L. Hartwell, *Mol. Cell. Biol.* **15**, 6128 (1995).
10. L. Ross, C. I. Nugent, V. Lundblad, data not shown.
11. D. Lydall and T. Weinert, *Science* **270**, 1488 (1995).
12. C. Nugent and V. Lundblad, unpublished observations.
13. J. Parenteau, R. Wellinger, V. Lundblad, data not shown. The limits of this assay are such that a minor increase in short stretches of single-strand DNA would not be detectable in the *cdc13-2^{est}* mutant.
14. The *cdc13-2^{est}* mutation is a $Glu^{252} \rightarrow Lys$ change, and the *cdc13-1^{ts}* mutation is a $Pro^{371} \rightarrow Ser$ change (*10*).
15. Telomeres were slightly longer in the *cdc13-1^{ts}* strain at 23°C, as previously observed (*9*). This implies that some aspect of negative regulation of telomere length control has been affected; we do not yet know the mechanism.
16. L. H. Hartwell and D. Smith, *Genetics* **110**, 381 (1985).
17. M. Cohn and E. H. Blackburn, *Science* **269**, 396 (1995).
18. For preparation of extracts, 2 liters of late log-phase culture were harvested and resuspended in an equal volume of lysis buffer (*26*); 10 ml of cell suspension was then mixed with an equal volume of glass beads in a 50-ml screw-cap centrifuge tube. The mixtures were vortexed repeatedly for 20 s at maximum speed followed by 20 s of cooling in an ice-water bath. The total vortexing time was ~10 min. Extracts were clarified by centrifugation at 10,000*g* for 10 min and then at 200,000*g* for 1 hour. Telomerase-containing fractions were derived from a POROS 50 HS column (PerSeptive Biosystems).
19. The wild-type Cdc13 and mutant Cdc13^{est} proteins, each with six histidines following the start methionine, were produced in Sf9 cells with the use of a baculovirus expression system (Gibco). After lysis by sonication, protein was isolated by affinity purification on Ni–nitrilotriacetic acid agarose (Qiagen); 10% glycerol and 0.5% Tween-20 were added to all protein buffers. Protein immunoblot analysis with antisera to the $(His)_6$ epitope (*27*) confirmed that the purified protein was Cdc13p (*20*).
20. T. Hughes and V. Lundblad, unpublished observations.
21. Three independent assays measured the degree of competition for binding to labeled $d(TGTGTGGG)_3$ oligomer in the presence of 1:1 and 10:1 molar excess of yeast, human, and *Oxytricha* cold competitor DNAs; data were quantitated by PhosphorImager analysis.
22. Overexpression of wild-type *EST1* suppresses the *cdc13-2^{est}* mutation but not the *cdc13-1^{ts}* mutation, and suppression is specific for the *EST1* gene, in that overexpression of *TLC1* or *EST2* has no effect (*12*).
23. V. Virta-Pearlman, D. K. Morris, V. Lundblad, in preparation.
24. D. E. Gottschling and V. A. Zakian, *Cell* **47**, 195 (1986); C. M. Price and T. R. Cech, *Genes Dev.* **1**, 783 (1987); J. T. Gray, D. W. Celander, C. M. Price, T. R. Cech, *Cell* **67**, 807 (1991); M. E. Cardenas, A. Bianchi, T. de Lange, *Genes Dev.* **7**, 883 (1993); H. Sheng, Z. Hou, T. Schierer, D. L. Dobbs, E. Henderson, *Mol. Cell Biol.* **15**, 1144 (1995).
25. N. W. Kim *et al.*, *Science* **266**, 2011 (1994); W. E. Wright, D. Brasiskyte, M. A. Piatyszek, J. W. Shay, *EMBO J.* **15**, 1734 (1996).
26. N. F. Lue and J. C. Wang, *J. Biol. Chem.* **270**, 21453 (1995).
27. H. Zentgraf *et al.*, *Nucleic Acids Res.* **23**, 3347 (1995).
28. Haploid strains for analysis were generated from either *cdc13-2^{est}/CDC13*, *tlc1-Δ::LEU2/TLC1* or *cdc13-1^{ts}/CDC13*, *tlc1-Δ::LEU2/TLC1* diploids constructed by gene replacement of a single wild-type diploid parental strain; all haploid strains used in Fig. 1 were isogenic. For Southern blot analysis, strains were grown from freshly germinated spores to saturation, followed by two successive subculturings, representing a total of ~50 generations of growth, before preparation of DNA.
29. E. J. Louis and J. E. Haber, *Genetics* **124**, 533 (1990); V. Lundblad and E. H. Blackburn, *Cell* **73**, 347 (1993).
30. The length of three individual telomeres (a 2.8-kb fragment corresponding to the left telomere of chromosome V-L and the 2.3- and 2.0-kb telomeres indicated by the lower two arrows in Fig. 1A) was measured by simultaneously probing with a telomere-specific probe and a λ-specific probe to detect diluted λHind III + λSty I markers present in each lane. The data are presented as the change between the "1x" and "3x" culture, rather than the change per cell generation, because of the rapid increase in dying cells in later cultures (which can still contribute DNA to the Southern profile). To ensure that similar numbers of cells were assayed over this time period, we assayed total cell counts for each successive culture; the variation between the three strains at each time point was no more than 20%.
31. Binding reactions were performed in 10 mM Hepes

(pH 7.8), 75 mM KCl, 2.5 mM $MgCl_2$, 0.1 mM EDTA, 1 mM dithiothreitol, 3% Ficoll, and polydeoxyinosinic-deoxycytidylic acid [poly(dI-dC)] (100 μg/ml). Protein and oligomers were added sequentially at 5-min intervals, incubated for 5 to 10 min at room temperature, and electrophoresed through a 5% nondenaturing polyacrylamide gel in 1× tris-borate EDTA at 200 V. Single-strand oligomers were heat-denatured and snap-cooled on ice to minimize the formation of secondary structures. In competition assays, labeled oligomers were mixed with the indicated molar excesses of unlabeled competitor before heat denaturation. Duplex oligomers were annealed in 50 mM NaCl by heating to 95°C for 2 min and cooling to ambient temperature over a 60-min interval before the binding assay; results for K_A assays were independent of which strand was labeled. In K_A assays, reactions were incubated on ice for 30 to 60 min and gels were run at 4°C; reactions for substrates 1 to 9 did not contain poly(dI-dC). Protein concentration was determined by amino acid analysis and by quantitative comparison to bovine serum albumin standards using SDS–polyacrylamide gel electrophoresis (PAGE) followed by Coomassie staining, which gave comparable results (within 15%). Coomassie gels and gel shifts were quantitated with a scanning densitometer or PhosphorImager, respectively, and the Imagequant software package (Molecular Dynamics).

32. R. J. Wellinger, A. J. Wolf, V. A. Zakian, *Cell* **72**, 51 (1993); R. J. Wellinger, K. Ethier, P. Labrecque, V. A. Zakian, *ibid.* **85**, 423 (1996).

33. We thank H. Zentgraf for monoclonal antibody 13/45/31, A. Salinger and K. Shah for technical assistance, and S. Elledge and S. Plon for critical review of the manuscript. Supported by grants from NIH and Geron Corporation and by an American Cancer Society Junior Faculty Research Award to V.L. T.R.H. is supported by an NIH predoctoral fellowship.

26 June 1996; accepted 13 September 1996

Visualization of Gene Expression in Living Adult *Drosophila*

Manuel Calleja, Eduardo Moreno, Soraya Pelaz, Ginés Morata*

To identify genes involved in the patterning of adult structures, Gal4-UAS (upstream activating site) technology was used to visualize patterns of gene expression directly in living flies. A large number of Gal4 insertion lines were generated and their expression patterns were studied. In addition to identifying several characterized developmental genes, the approach revealed previously unsuspected genetic subdivisions of the thorax, which may control the disposition of pattern elements. The boundary between two of these domains coincides with localized expression of the signaling molecule wingless.

The adult structures of *Drosophila* are subdivided into compartments in which patterning and growth are controlled by the heritable activities of selector genes (*1*) and by signals generated as a result of interactions between cells across compartment boundaries (*2*). However, there are few compartments; each segment is subdivided into anterior and posterior compartments, and only thoracic segments are further subdivided into dorsal and ventral and possibly trunk and appendage compartments (*3*). These compartments define large domains, which ultimately are composed of thousands of cells; little is known about how they are further subdivided genetically. Adult structures are differentiated by "imaginal" cells, which proliferate after the larval patterns are completed (*4*). Whereas a great deal is known about the genetic cascade [see (*5*) for an overall description] leading to generation of larval patterns, much less is known about the genetics of pattern formation in the adult, although progress recently has been made concerning how appendages develop (*2, 6*). Some genes are used during both embryogenesis and imaginal development, but others such as *vestigial* (*vg*), *apterous* (*ap*), *nubbin* (*nub*), *Dorsal wing* (*Dlw*), and *fringe* (*frg*) have their primary role in the adult (*7*), indicating that adult patterns have their own specificity.

To search for specific adult pattern genes, we modified the Gal4 enhancer trap method (*8*) so that we can observe the consequences of Gal4 activity directly in living flies. Our approach uses an upstream activating site (UAS) construct (*9*) containing the cDNA of the *yellow* (y) gene. The gene y is responsible for the normal pigmentation of adult cuticle and bristles all over the body. Flies mutant for *yellow* (y^-) are of yellow color and are clearly distinct from the wild type. The y^- mutations traditionally have been used as gratuitous markers in genetic mosaic experiments and do not affect viability or fertility. Flies that express Gal4 will express the y^+ product under control of the UAS. When expressed in a y^- fly, the body domain in which the y^+ gene is turned on by Gal4 will appear as a patch of y^+ territory on a y^- background, and this y^+ tissue will be detectable under the dissecting microscope.

To determine the developmental period in which the Gal4 product has to be present to produce detectable y^+ rescue, we used a *hsp70-GAL4* construct (*10*) to induce controlled synthesis of the Gal4 product. Single 90-min pulses were given to different batches of *hsp70-GAL4/UAS-y* larvae or pupae grouped according to age with respect to the time of puparium formation, and the emerging adults were inspected for y^+ rescue. Heat shocks given at or after the second half of the third larval period are able to produce y^+ rescue. All genes known to be involved in the patterning of adult structures are expressed at the end of the third larval instar (*2, 6, 7*). Thus, y^+ expression under Gal4 control should be able to detect gene expression not only during late pupal stages when the adult cuticle is being formed but also much earlier when patterning genes are active. Our finding of insertions in several known developmental genes (see below) supports this notion.

We mobilized the transposon *pGawB* (*11*), a Gal4-containing *P* element (*8*), to produce lines that express Gal4 in a manner that reflects the expression pattern of the genes where the transposon inserted. Each insertion was tested indiscriminately in a cross with the *UAS-y* gene construct. Of 1020 insertions, 447 (44%) gave partial or total y^+ rescue in adult flies (see Table 1 for details and different classes of expression). However, the majority of the lines failing to give y^+ rescue correspond to insertions in which the *GAL4* gene is inactive, as more than 90% of them (56 from a sample of 59) also fail to show any embryonic expression when tested with a *UAS-lacZ* construct (*8, 12*). Considering only those lines in which the *pGawB* is active, about 90% of them produce detectable y^+ rescue in adult flies. The implication is that the majority of the *Drosophila* genes are expressed in imaginal cells and are detectable by our method.

We are interested in the lines with y^+ rescue that is restricted to specific and well-delimited body regions (Table 1). These lines contain insertions in genes that may be involved in developmental processes specific to the structures in which they are expressed. Moreover, these lines can provide information about how adult patterns are genetically subdivided. An additional technical advantage of the screen is that it provides a collection of Gal4 driver lines that express Gal4 strongly enough to yield detectable adult expression and therefore are very useful in gene-targeting experiments.

We isolated 27 lines that express y^+ in a region-specific manner. Nine of them were later found to be insertions in known developmental genes (*13*): *Distal-less* (*Dll*), *caudal* (*cad*), *apterous* (*ap*), *optomotor-blind*

Centro de Biología Molecular, Universidad Autónoma de Madrid, Consejo Superior de Investigaciónes Científicas, Madrid 28049, Spain.

*To whom correspondence should be addressed. E-mail: gmorata@mvax.cbm.uam.es